Bulletin of Pure and Applied Science
Physics, Vol.41D No.2,
July-December 2022 P.75-80
Original Research Article

Print version ISSN 0970 6569
Online version ISSN 2320 3218
DOI: 10.5958/2320-3218.2022.00014.8
Available online at www.bpasjournals.com

Radiation Leakage Images For Two Different Dielectric-Loaded Surface Plasmon Polariton Waveguides

[1]Jay Shankar Kumar*, [2]Ashok Kumar

Author's Affiliations:
[1]Research Scholar, University Department of Physics, B.N. Mandal University, Madhepura, North Campus, Singheshwar, Bihar 852128, India.
E-mail: jayphysics108@gmail.com
[2]University Department of Physics, B.N. Mandal University, Madhepura, North Campus, Singheshwar, Bihar 852128, India.
E-mail: ashokabnu@yahoo.co.in

***Corresponding author:**
Jay Shankar Kumar
Research Scholar, University Department of Physics, B.N. Mandal University, Madhepura, North Campus, Singheshwar, Bihar 852128, India.
E-mail: jayphysics108@gmail.com

Received on 26.05.2022
Revised on 21.09.2022
Accepted on 29.10.2022
Published on 15.12.2022

ABSTRACT

We have studied about leakage radiation images obtained for two different dielectric-loaded surface plasmon polariton waveguides based on routing structures; linear couplers and bent waveguides. By simultaneously imaging the conjugated aperture and field planes of the microscope, we unambiguously quantify the degeneracy lift occurring for strongly interacting dielectric loaded surface plasmon polariton waveguides and visualize the symmetry of the coupled modes. We have obtained the wave vector distribution and showed its evolution with the bend radius. We have developed a numerical and an analytical analysis for momentum distribution. We have found that for large radii i.e. for vanishing bending loss, we can link the plasmon in Fourier space with the geometrical and modal properties of the bend structure. It was also found that the radial dependence of the wave vector distribution is governed by the phase difference. The obtained results were found in good agreement with previously obtained results.

KEYWORDS

Radian leakage, dielectric, surface plasmon, polariton, wave guide, routing structure, degeneracy, Fourier space.

How to cite this article: Kumar J.S., Kumar A. (2022). Radiation Leakage Images For Two Different Dielectric-Loaded Surface Plasmon Polariton Waveguides. *Bulletin of Pure and Applied Sciences- Physics,* 41D (2), 75-80.

INTRODUCTION

The different geometries capable of routing the flow of surface plasmons, dielectric loaded surface plasmon polariton wave-guides [1-3] have emerged as a potential plasmonic architecture that can be integrated seamlessly with current silicon on insulator photonic circuits [4,5] and can sustain transfer of information at high date rates [6]. A dielectric loaded surface plasmon polariton loaded surface plasmon polariton waveguide is made of a rectangular dielectric rib deposited on a metal film or strip [7]. The surface plasmon required for an optimum confinement of the mode compare well with state of the art silicon on insulator waveguides operating in the telecom bands. Despite higher losses, the advantage of such a plasmonic platform is that the optical index of the dielectric material used to confined the mode can be controlled extremely to realize active dielectric loaded surface plasmon polariton waveguide-based devices [8-12]. Near field optical microscopy and far field leakage radiation microscopy [13] are instrumental for visualizing the confinement and propagation details of surface plasmons supported by this geometry [14,15]. For thin metal films, leakage radiation microscopy is an especially useful characterization tool. Effective indices of the different modes and interactions developing in a given structure can be readily determined [16-18].

METHOD

Optical characterization is performed by using homemade leakage radiation microscopy. An incident tunable laser beam is focused by 100x microscope objective on the extremity of a dielectric loaded surface plasmon polariton waveguide. The sharp discontinuity by the polymer structure acted a local scatterer and produced a spread of wave vectors, some of which resonated with the surface plasmon modes supported by the geometry. By controlling the incident polarization parallel to the longitudinal axis of the waveguide, the dielectric loaded surface plasmon polariton waveguide mode can readily be excited. The leakage radiation microscopy provided a far field imaging technique to directly visualized surface plasmon propagation. This method relies on the collection of radiation losses occurring in the waveguide during propagation. These losses were emitted in the substrate at an angle phase matched with the in plane wave vector of the surface plasmon polariton mode. In our leakage radiation microscopic, the plasmon radiation losses were collected by an oil-immersion objective with numerical aperture. the plane provided direct information about the propagation of the surface plasmon mode developing in dielectric loaded surface plasmon polariton waveguide. To complete the analysis we have used the Fourier transforming property of the ovbjective to access the wave vector distribution of the emitted light. The angular distribution of the radiation in the substrate collected by the object transformed to a lateral distribution at the objective back focal plane. We obtained the quantitative result of the complex surface plasmon wave vector in complex effective index consisting of the radial distance with respect to optical axis. Access to momentum space was performed by inserting a beam splitter in the optical path and a set of Fourier transforming relay. The obtained results were compared with previously obtained results.

RESULTS AND DISCUSSION

Graph (1) (a) and graph (1)(b) show images of the leakage radiation intensity of a single mode dielectric loaded surface plasmon polariton waveguide in conjugated image and Fourier planes respectively. The plasmon mode was launched at the bottom of the structure and propagated up the waveguide with an exponentially decaying intensity. The image of graph (1)(b) is the wave vector content of the intensity distribution shown in graph (1)(a). Both Fourier plane and image plane images, a calibration was performed prior to any data extraction. For calibrating image plane images we have used the known waveguide length as a standard with the system magnification, one pixle represents $\square\ 0.6\mu m$. For Fourier plane

images the numerical aperture of the objective was used. The largest ring in graph (1)(b) represents the numerical aperture 1.49 specified. The central disc is the numerical aperture of the x100 excitation objective at numerical aperture 0.52. On pixle provided a $\Delta N.A \square 0.012$. The dielectric loaded surface plasmon polariton waveguide mode propagating along this straight waveguide is shown in graph (3). The Fourier plane image is shown in graph (1)(b) contains more information than a direct space image since the real part and imaginary part of the effective index can be obtained directly. The mode is represented by a single line at a constant $n_{eff} = \frac{k_y}{k_0} = 1.262 \pm 0.006$. The intensity along $\frac{k_y}{k_0}$ at $k_x = 0$ is related to the surface plasmon through the following formula:

$$I\left(k_x, k_y\right) \alpha \left|\tilde{H}_0\left(k_x\right)\right|^2 / \left[\left(k_y - \beta'\right)^2 + \left(1/2L_{spp}\right)^2\right]$$

$H_0\left(k_x\right)$ is the k_x Fourier transform of the guided magnetic field at the objective focal point. The imaginary party of the effective index was estimated precisely through a Lorentzian fit. Graph (2) shows the benefit of performing momentum spectroscopy. Grpah (2)(a) and (2)(b) are leakage radiation images obtained at the conjugated Fourier plane and image plane for a linear coupler with d=440nm. The coupling length L_C was evaluated using the relation

$$L_c = \frac{\pi}{\left|\beta_s^{'} - \beta_{as}^{'}\right|}$$

Where $\beta_s^{'} = k_0 \times n_{eff}^{s}$ and $\beta_{as}^{'} = k_o \times n_{eff}^{as}$. then

$$L_c = \frac{\lambda_0}{2\left|n_{eff}^{s} - n_{eff}^{as}\right|} = 15.2\mu m$$

We have proposed a simple analytical model that explains the main features of obtained Fourier plane images. We have approximated the mode that propagated in the bend structure by a Guassian profile with a finite propagation length. To simulate the curved dielectric loaded surface plasmon polariton waveguide we have maintained the complex propagation constant in the curved section equal to that of the straight waveguides. The assumption remained valid for $R_c > R_l$ where R_l is the liming radius where bend losses can be neglected. Graph (3) shows the impact of the integration boundaries on the momentum space representation of a single straight wave guide for a fixed propagation length of 40 µm. There is a perfect agreement between numerically calculated Fourier transform and its analytical solution. For integration boundries greater than the propagation length, the two calculations matched with the Lorentz function which are generally used. The obtained results were compared with previously obtained results of theoretical and experimental research works and were found in good agreement.

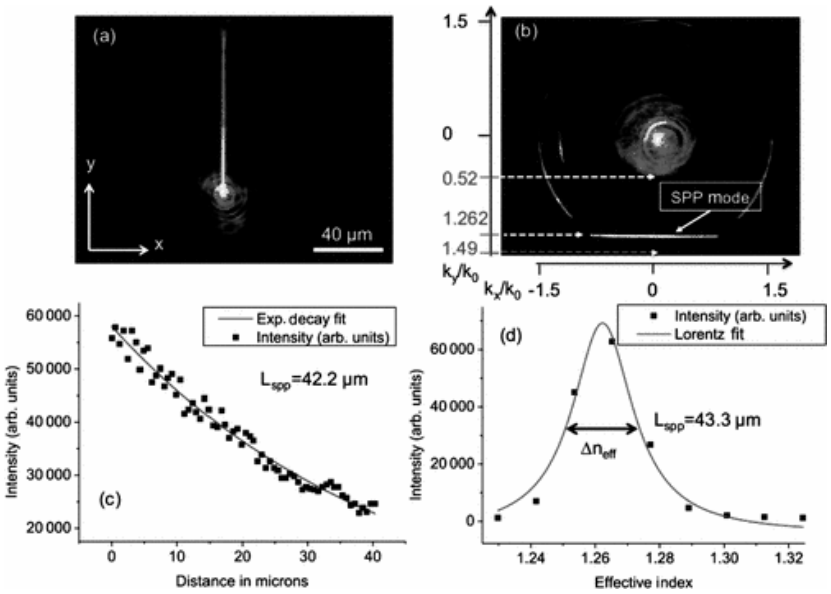

Graph 1: (a) Intensity distribution at the image plane of a surface plasmon mode propagating along a straight dielectric loaded surface plasmon polariton waveguide. The excitation spot is readily visible at the lower portion of the waveguide. (b) Corresponding wave-vector distribution. The central disk represents the numerical aperture of the illumination objective (0.52). The dielectric loaded surface plasmon polariton mode is recognized as a bright line at constant k_y / k_x.

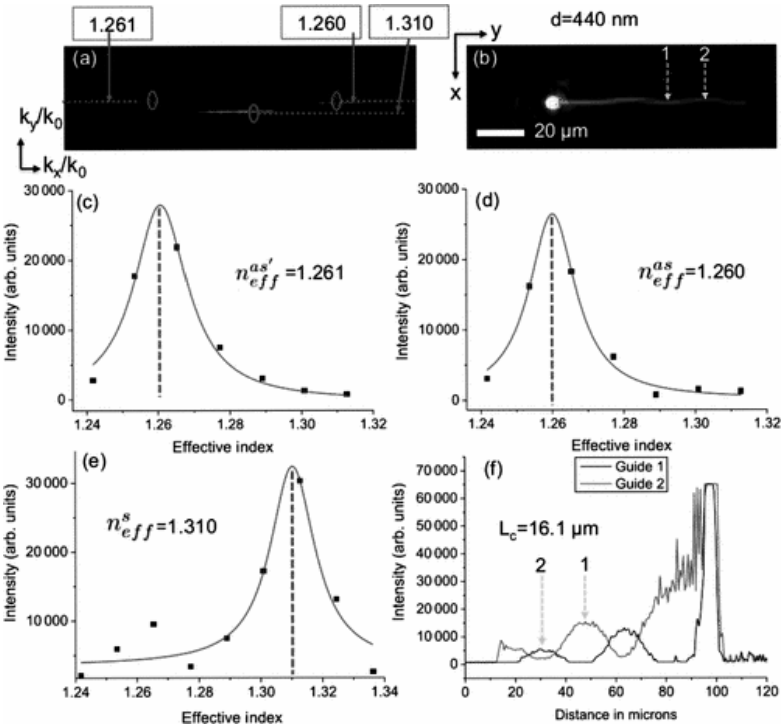

Graph 2: (a)+(b) are leakage radiation Fourier and image planes obtained from a linear Dielectric loaded surface plasmon polariton waveguide coupler width d =440nm. (c) and (d) are Lorentzian fits of the asymmetric mode at the location marked by the circle in (a). (e) is a Lorentzian fit of the symmetric mode. (f) Longitudinal intensity cross sections taken along the two cupled waveguides in (b) showing the energy transfer from one Dielectric loaded surface plasmon polariton waveguide to the other defining the coupling length L_c.

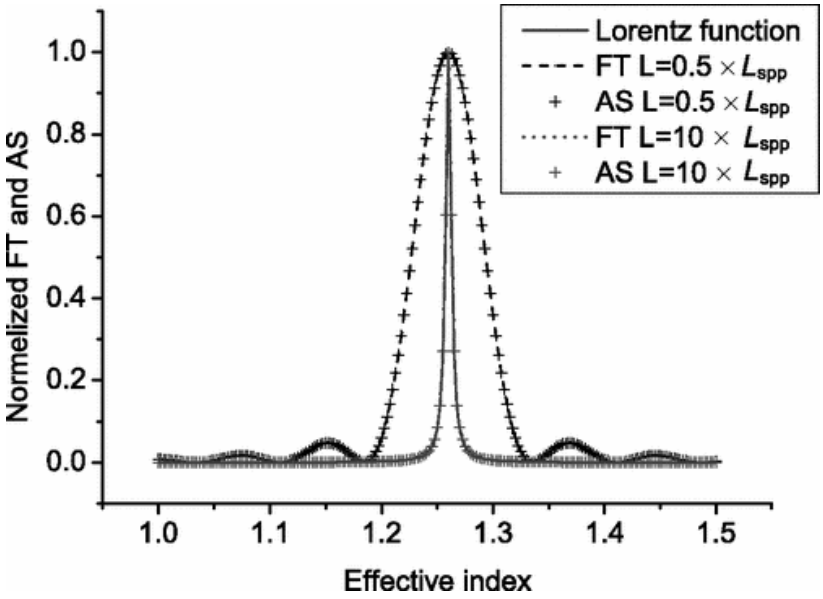

Graph 3: Effect of the Dielectric loaded surface plasmon polariton waveguide length on Fourier-plane calculations. Dashed line: calculated Fourier plane (FT) cross section for $L = 0.5 \times L_{spp}$ and $L = 10 \times L_{spp}$.

CONCLUSION

We have studied the leakage radiation images obtained for two different dielectric loaded surface plasmon polariton waveguides based on routing structures. We have analysed the energy transfer between coupled waveguides as function of gap distance and revealed the momentum distribution of curved geometries. We have found a clear degeneracy lift of the effective indices for strongly interacting waveguides in agreement with coupled mode theory. We have found that for large radii, we can link the plasmon in Fourier space with the geometrical and modal properties of the band structure. The radial dependence of the wave vector distribution was governed by phase difference. This corresponds to the resonance condition of a ring resonator. We have considered each part of the waveguide straight and bend independently from each other. The straight parts were approximately 30μm long, a length smaller than the longitudinal decay of the supported mode. For a long waveguide no oscillation of the wave vector distribution was found. The obtained results were found in good agreement with previously obtained results.

REFERENCES

[1] A. Honenau, J. R. Krenn, A. L. Stepanov. et al, Opt. Lett. 30, 893, (2005).
[2] T. Holmgaad, S. I. Bozhevolnyi, L. Markey and A. Dereux. Appl. Phys. Lett. 92, 011124, (2008).
[3] J. Grandidieretal, Phys. Rev. B. 78, 245419, (2008).
[4] R. M. Briggs, et al., Nano Lett. 10, 4851, (2010).
[5] D. Kalavrouziotis et al., IEEE, Photonics Technol, Lett. 24, 1036, (2012).
[6] S. Papaionannou et al., IEEEJ, Light Wave Technol. 29, 3185, (2011).
[7] J. Grandidier, G. Colas des Francs, L. Markey, A. Bouhelier, S. Massenot, J. C. Weeber and A. Dereux, Appl. Phys. Lett. 96, 063105, (2010).
[8] J. Gosciniak, S. I. Bozhenvolnyi et al., Opt. Express 18, 1207, (2010).
[9] S. Randhawa et al., Opt. Express, 20, 2354, (2012).
[10] D. Perron, M. Wu, C. Horvath, D. Bachman and V. Van, Opt. Lett. 36, 2731, (2011).
[11] A. V. Krasavin, S. Randhawa, J. S. Bouillard, J. Renger, R. Quidant and A. V. Zayats, Opt. Express. 19, 25222, (2011).
[12] K. Hassan, J. C. Weeber, L. Markey and A. Dereux, J. Appl. Phys. 110, 023106, (2011).

[13] B. Hecht, H. Bielefeldt, L. Novotny, Y. Inouye and D. W. Pohl, Phys. Rev. Lett. 77, 1889, (1996).

[14] T. Holmgaard et al. Phys. Rev. B, 78, 165431, (2008).

[15] B. Steinberger, A. Hohenau et al., Appl. Phys. Lett. 91, 081111, (2007).

[16] A. Krishnan, C. J. Regan, L. G. De peralta and A. A. Bernussi, Appl. Phys. Lett. 97, 231110, (2010).

[17] J. Berthelot, A. Bouhelier, G. Colasdes Francs, J. C. Weeber and A. Dereux, Opt. Express. 19, 5303, (2011).

[18] C. J. Regan, O. Thiabgoh, L. G. De Peralta and A. Bernussi, Opt. Express, 20, 8658, (2010).

****